Weierstraß-Institut

für Angewandte Analysis und Stochastik

Leibniz-Institut im Forschungsverbund Berlin e. V.

Preprint ISSN 2198-5855

Longitudinal modes of multisection ring and edge-emitting semiconductor lasers

Mindaugas Radziunas[1]

submitted: October 15, 2014

[1] Weierstrass Institute
Mohrenstr. 39
10117 Berlin, Germany
E-Mail: Mindaugas.Radziunas@wias-berlin.de

No. 2011

Berlin 2014

2010 *Mathematics Subject Classification.* 78-04 78A60 35-04 78-05.

2008 *Physics and Astronomy Classification Scheme.* 42.55.Px 42.60.-v 02.30.Jr 02.60.Cb.

Key words and phrases. traveling wave mode, semiconductor laser, optical mode, mode analysis.

This work is supported by EU FP7 ITN PROPHET, Grant No. 264687.

Edited by
Weierstraß-Institut für Angewandte Analysis und Stochastik (WIAS)
Leibniz-Institut im Forschungsverbund Berlin e. V.
Mohrenstraße 39
10117 Berlin
Germany

Fax: +49 30 20372-303
E-Mail: preprint@wias-berlin.de
World Wide Web: http://www.wias-berlin.de/

Abstract

We use the traveling wave model for simulating and analyzing nonlinear dynamics of multisection ring and edge-emitting semiconductor laser devices. We introduce the concept of instantaneous longitudinal optical modes and present an algorithm for their computation. A semiconductor ring laser was considered to illustrate the advantages of the mode analysis.

1 Introduction

Multisection semiconductor edge-emitting and ring lasers (MSLs) are interesting devices for different applications. Different mathematical models are used for simulation of dynamics of MSLs. The models range from simple ODE or DDE systems (rate equations) to 2+1 or 3+1 dimensional PDEs. Simple ODE and DDE models usually are based on mean-field approximations and take into account only a few basic characteristics of the considered lasers or are suited to describe particular MSL configurations [1, 2]. On the other hand, simulations of much more precise multidimensional PDE models [3] are time-consuming, while application of analytic methods becomes much more difficult.

Traveling Wave (TW) model [4, 5] is a compromise between simplicity and precision. It is a 1+1-dimensional PDE system describing dynamics of longitudinal distributions of counter-propagating slowly varying optical fields, polarization functions and carrier density. This modeling can take into account optical injections, field reflections and transmissions at the interfaces of different laser parts, as well as delayed feedback of the optical fields. Comparing to ODE and DDE models mentioned above, the TW model is computationally more demanding but still enables an advanced analysis. The main aim of this paper is to introduce the basic structural elements of our model, to explain the construction of different laser devices from these elements, to present an algorithm for computation of the instantaneous modes of MSLs, and to demonstrate the application of these modes for analysis of different operation regimes of MSLs.

2 Model of the MSL

For simulations and analysis of MSLs, we apply our software kit `LDSL-tool` [6]. It allows to consider a large variety of laser devices or coupled laser systems that can be schematically represented by a set of mutually interconnected *sections* $S_k|_{k\in\{1,\dots,n\}}$ and *junctions* $J_l|_{l\in\{1,\dots,m\}}$. According to our laser device construction, for any edge of any of n sections we can attribute a unique junction. On the other hand, at least a single edge of some section joins each of m

junctions J_l (see Fig. 1 where schemes of a few typical MSLs are presented). At the junctions representing laser facets, we can apply one or several optical injections (panel (c)) and record the emitted optical fields (panel (d)).

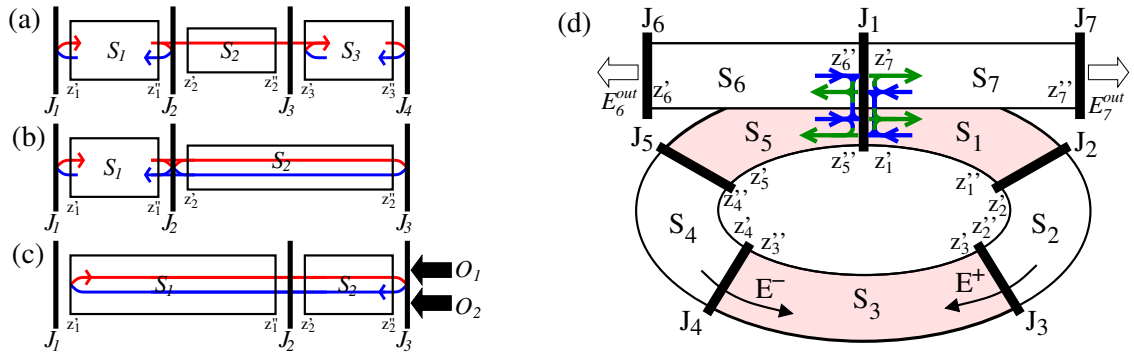

Figure 1: Schemes of MSLs with an indication of sections S_k (bounded areas), junctions J_l (thick bars), optical injections O_i (thick black arrows), and emitted fields (thick empty arrows). Thin arrows show field propagation and transmission - reflection - out-coupling directions. (a): Master-Slave laser system. (b): Laser with a delayed optical feedback. (c): Two section mode-locked laser with dual optical injection. (d): Ring MSL with an out-coupling waveguide.

Each laser section $S_k|_{k\in\{1,\dots,n\}}$ is identified with a unique spatial interval (z_k', z_k''), where z_k' and z_k'' ($z_k', z_k'' \in \mathbf{R}$, $z_k'' > z_k'$) are the spatial coordinates of the section edges (see Fig. 1) and $|S_k| = z_k'' - z_k'$ is the length of S_k. Within each laser section the field equations [4]

$$-i\partial_t \Psi(z,t) = \mathcal{H}(\beta^{\pm})\Psi + \mathcal{F}_{sp}, \qquad \beta^{\pm}(z,t) = \bar{\beta}(z,t) \pm \Delta_\beta(z,t),$$
$$\mathcal{H} = \begin{pmatrix} v_g H_0(\beta^{\pm}) + \frac{iv_g g_p}{2}\mathcal{I} & -\frac{iv_g g_p}{2}\mathcal{I} \\ -i\gamma_p \mathcal{I} & (i\gamma_p + \omega_p)\mathcal{I} \end{pmatrix}, \quad H_0 = \begin{pmatrix} i\partial_z - \beta^+ & -\kappa^- \\ -\kappa^+ & -i\partial_z - \beta^- \end{pmatrix} \tag{1}$$

govern the spatial-temporal dynamics of the four-component wave function $\Psi(z,t) = \binom{E}{p}$, where $E = \binom{E^+}{E^-}$ and $p = \binom{p^+}{p^-}$ denote slowly varying counter-propagating optical fields and polarizations, respectively. Here, $\mathcal{I}$ is the 2×2 identity matrix, v_g is the group velocity, g_p, $2\gamma_p$, and ω_p are the amplitude, the width and the relative central frequency of Lorentzian approximation of the frequency dependent gain close to its maximum [4], and $\mathcal{F}_{sp}$ models the spontaneous emission. The complex factors $\kappa^{\pm}(z)$ represent the distributed backscattering of the fields due to, e.g., Bragg grating. Finally, β^+ and β^- are the complex propagation factors for forward- and backward-propagating fields, respectively. Since we do not exploit the dependence of $\beta^{\pm}$ on the carriers in this paper, we skip a more detailed description of $\beta^{\pm}$ and refer to [4, 7] instead. Note only, that in contrast to linear MSLs the asymmetry factor Δ_β in ring lasers is non-vanishing and is mainly imposed by the dominance of the cross-gain over the self-gain saturation [2]. Thus, in the sequel we use a pure imaginary Δ_β, which for $|E^{\pm}|^2 \gg |E^{\mp}|^2$ reads as $\Delta_\beta = \pm i|\Delta_\beta|$.

To complete the TW model (1), one needs to relate the fields that are entering and leaving all laser sections. Assume that any junction J_l connects the left edges $z'_{l'_r}$ (right edges $z''_{l''_r}$) of the sections $S_{l'_r}$ ($S_{l''_r}$), and all such indices l'_r (l''_r) are components of the vector $\vec{l}'$ ($\vec{l}''$). Let $|\vec{l}'|$ and $|\vec{l}''|$ be the number of components in the corresponding vector, so that the total number of the

section edges connected to J_l is $|\vec{l}|=|(\vec{l}'_{\vec{l}''})|=|\vec{l}'|+|\vec{l}''|\geq 1$. Note also, that all junctions together connect all $2n$ section edges: $\sum_{l=1}^{m}|\vec{l}|=2n$. If needed, one can also assume $|\vec{l}^{\,i}|\geq 0$ optical injections $O_{l_r^i}$ applied to some section edges joining J_l and record the emission E_l^{out}. According to our modeling approach, the required optical fields $E^+_{\vec{l}'}$ and $E^-_{\vec{l}''}$ entering laser sections at any J_l, as well as the emission E_l^{out} are determined by complex $|\vec{l}|\times|\vec{l}|$, $|\vec{l}|\times|\vec{l}^{\,i}|$, and $1\times(|\vec{l}|+|\vec{l}^{\,i}|)$ dimensional matrices $\mathcal{T}_l$, $\mathcal{T}_l^i$ and $\mathcal{T}_l^o$:

$$\begin{gathered}\begin{pmatrix}E^+_{\vec{l}'}\\ E^-_{\vec{l}''}\end{pmatrix}=\mathcal{T}_l\begin{pmatrix}E^+_{\vec{l}''}\\ E^-_{\vec{l}'}\end{pmatrix}+\mathcal{T}_l^i O_{\vec{l}^{\,i}},\quad E_l^{\rm out}=\mathcal{T}_l^o\begin{pmatrix}E^+_{\vec{l}''}\\ E^-_{\vec{l}'}\\ O_{\vec{l}^{\,i}}\end{pmatrix},\quad \text{where}\\ E^\pm_{\vec{l}'}=\begin{pmatrix}E^\pm(z'_{l'_1},t)\\ \vdots\\ E^\pm(z'_{l'_{|l'|}},t)\end{pmatrix},\quad E^\pm_{\vec{l}''}=\begin{pmatrix}E^\pm(z''_{l''_1},t)\\ \vdots\\ E^\pm(z''_{l''_{|l''|}},t)\end{pmatrix},\quad O_{\vec{l}^{\,i}}=\begin{pmatrix}O_{l^i_1}(t)\\ \vdots\\ O_{l^i_{|l^i|}}(t)\end{pmatrix}.\end{gathered}\tag{2}$$

3 Instantaneous optical modes

The *instantaneous* optical modes of MSLs are pairs $(\Omega(\beta^\pm),\Theta(z,\beta^\pm))$ of complex eigenvalues and eigenvectors of the spectral problem defined by Eq. (2) and the field operator $\mathcal{H}(\beta^\pm)$ from (1) determined at *instantaneous* distributions $\beta^\pm(z,t)$ [8]. The imaginary and the real parts of Ω are mainly defining the angular frequency and the damping of the mode. The four-component vector-eigenfunction $\Theta=\binom{\Theta_E}{\Theta_p}$ with $\Theta_\upsilon=\binom{\Theta^+_\upsilon}{\Theta^-_\upsilon}$ and $\upsilon=E,p$ determines the spatial distribution of the mode. Note also, that any stationary state of the MSL is determined by an optical mode $(\bar\omega,\Theta(z))$ with a *real* frequency $\bar\omega$: $\Psi(z,t)=\Theta(z)e^{i\bar\omega t}$.

Let us consider an arbitrary MSL with no optical injections. For any fixed $\beta^\pm(z)$ the substitution of $E(z,t)=\Theta(z,\beta^\pm)e^{i\Omega t}$ into Eq. (1) and the elimination of $\Theta_p^\pm$ imply a linear system of ODEs for $\Theta_E^\pm(z)$ within each section $S_k|_{k\in\{1,\dots,n\}}$. The solution of this system in each laser section can be written as

$$\begin{gathered}\Theta_E(z,\beta^\pm)=e^{-i\int_{z'}^{z}\Delta_\beta(\xi)d\xi}\,e^{i\int_{z'}^{z}\mathcal{D}(\bar\beta(\xi),\Omega)d\xi}\,\Theta_E(z',\beta^\pm),\qquad\text{where}\\ \mathcal{D}(\bar\beta,\Omega)\overset{def}{=}\begin{pmatrix}-\bar\beta-v_g^{-1}\Omega-\chi(\Omega) & -\kappa^-\\ \kappa^+ & \bar\beta+v_g^{-1}\Omega+\chi(\Omega)\end{pmatrix},\quad \chi(\Omega)\overset{def}{=}\tfrac{g_p}{2}\tfrac{\Omega-\bar\omega}{\gamma_p+i(\Omega-\omega_p)}.\end{gathered}$$

This expression together with the boundary conditions (2) for the mode functions $\Theta_E(z,\beta^\pm)$ give us $4n$ linear algebraic equations relating $4n$ mode function values $s_k'^\pm$ and $s_k''^\pm$ at both edges of all sections S_k, $k\in\{1,\dots,n\}$:

$$\begin{gathered}\begin{pmatrix}s''^+_k\\ s''^-_k\end{pmatrix}=e^{-i\langle\Delta_\beta\rangle_k}e^{i\langle\mathcal{D}(\bar\beta,\Omega)\rangle_k}\begin{pmatrix}s'^+_k\\ s'^-_k\end{pmatrix}\Big|_{k\in\{1,\dots,n\}},\quad\begin{pmatrix}s'^+_{\vec{l}'}\\ s''^-_{\vec{l}''}\end{pmatrix}=\mathcal{T}_l\begin{pmatrix}s''^+_{\vec{l}''}\\ s'^-_{\vec{l}'}\end{pmatrix}\Big|_{l\in\{1,\dots,m\}},\\ \langle y\rangle_k\overset{def}{=}\int_{S_k}y(z)dz,\quad s_k^{\nu\pm}\overset{def}{=}\Theta_E^\pm(z_k^\nu,\beta^\pm),\quad \nu\in\{\prime,\prime\prime\},\quad k\in\{1,\dots,n\},\\ \Rightarrow\quad\mathcal{M}\left(\Omega;\bar\beta,\Delta_\beta\right)\mathcal{S}=0,\ \ \mathcal{S}\overset{def}{=}\left(s_1'^+,s_1'^-,s_1''^+,s_1''^-,\dots,s_n'^+,s_n'^-,s_n''^+,s_n''^-\right)^T.\end{gathered}\tag{3}$$

Assume that the resulting system of $4n$ linear homogeneous equations determined by a sparse $4n\times4n$-dimensional complex matrix $\mathcal{M}$ remains linearly independent for almost all Ω. Nontrivial

solutions $\mathcal{S}$ (i.e., nontrivial eigenfunctions Θ of the spectral problem) will be available only for those Ω which are the complex roots of the following *characteristic* equation:

$$\det \mathcal{M}\left(\Omega; \bar{\beta}, \Delta_\beta\right) = 0. \tag{4}$$

All complex Ω solving Eq. (4) are eigenvalues of the spectral problem. A finite set of most important complex frequencies Ω is found by means of the Newton iteration and homotopy method based numerical algorithm [8].

4 Mode analysis of the ring laser

Let us consider the ring MSL shown in Fig. 1(d). Here, $n = m = 7$, whereas optical injections and matrices $\mathcal{T}_l^i|_{l\in\{1,\ldots,7\}}$ in (2) are absent. At J_1 Eqs. (2) are defined by

$$\left\{ \begin{array}{l} E^{\pm}_{\vec{1}'} = \begin{pmatrix} E^{\pm}(z_1', t) \\ E^{\pm}(z_7', t) \end{pmatrix} \\ E^{\pm}_{\vec{1}''} = \begin{pmatrix} E^{\pm}(z_5'', t) \\ E^{\pm}(z_6'', t) \end{pmatrix} \end{array} \right., \quad \mathcal{T}_1 = \begin{pmatrix} t_1 & i\tilde{t}_1 & -r_1^* & 0 \\ i\tilde{t}_1 & t_1 & 0 & 0 \\ r_1 & 0 & t_1 & i\tilde{t}_1 \\ 0 & 0 & i\tilde{t}_1 & t_1 \end{pmatrix}, \; t_1^2 + \tilde{t}_1^2 + |r_1|^2 \le 1,$$

where r_1 is a *localized* backscattering of the fields during coupling of the ring MSL to the output waveguide [2, 10]. Other vectors and matrices in (2) are given by

$$\begin{array}{l} E^{\pm}_{\vec{l}'} = E^{\pm}(z_l', t)|_{l\in\{2,\ldots,6\}}, \quad E^{\pm}_{\vec{l}''} = E^{\pm}(z_{l-1}'', t)|_{l\in\{2,3,4,5\}}, \quad E^{\pm}_{\vec{7}''} = E^{\pm}(z_7'', t), \\ E^{\pm}_{\vec{7}'} = E^{\pm}_{\vec{6}''} = \emptyset, \quad \mathcal{T}_{2,\ldots,5} = \mathcal{I}, \quad \mathcal{T}_6 = \mathcal{T}_7 = 0. \end{array}$$

In the sequel, we shall also assume vanishing distributed backscattering, $\kappa^{\pm} = 0$. The characteristic equation (4) for the ring MSL in this case can be written as

$$e^{i\langle\chi(\Omega_{k_\pm})\rangle} e^{i\langle\bar{\beta}\rangle} e^{i\tau\Omega_{k_\pm}} = t_1 \cosh|\langle\Delta_\beta\rangle| \pm \nu\sqrt{t_1^2 \sinh^2|\langle\Delta_\beta\rangle| - |r_1|^2}, \tag{5}$$

where $\langle y\rangle \stackrel{def}{=} \sum_{k=1}^5 \langle y\rangle_k$, $\tau = \langle v_g^{-1}\rangle$ is the field propagation time along the ring, $\nu = \pm 1$ is such that $\langle\Delta_\beta\rangle = i\nu|\langle\Delta_\beta\rangle|$, and $k_\pm$ are indices of the mode frequency pairs, Ω_{k_-} and Ω_{k_+}. The mode frequencies for small $\langle\chi(\Omega)\rangle$ and r_1 are related by

$$\begin{array}{l} \Omega_k \approx \Omega_0 + \frac{2\pi}{\tau}k, \quad \Omega_{k_+} - \Omega_{k_-} \approx \left\{ \begin{array}{ll} \frac{2\nu|r_1|}{\tau t_1} & \text{for } |\langle\Delta_\beta\rangle| < \Delta_0,\ \langle\Delta_\beta\rangle \to 0 \\ -\frac{2\nu|\langle\Delta_\beta\rangle|}{\tau} i & \text{for } |\langle\Delta_\beta\rangle| > \Delta_0 \end{array} \right., \\ \text{where} \qquad \Delta_0(r_1) \stackrel{def}{=} \ln\frac{|r_1| + \sqrt{t_1^2 + |r_1|^2}}{t_1}, \qquad |k| \in \{0, 1, \ldots\} \end{array} \tag{6}$$

For $|\langle\Delta_\beta\rangle| = \Delta_0$, one has a degenerate case of coinciding mode frequencies, $\Omega_{k_+} = \Omega_{k_-}$. Panels (a) and (b) of Fig. 2 show splitting of the complex frequencies Ω_{k_+} and Ω_{k_-} by non-vanishing $\langle\Delta_\beta\rangle$ and $|r_1|$, respectively. The distributions $\beta^{\pm}$ used for mode computations were obtained by numerical integration of full TW model [4]. The corresponding stationary and alternating oscillation states were governed by modes with zero or almost zero damping: see mode frequencies within small boxes in Fig. 2(a) and (b), respectively.

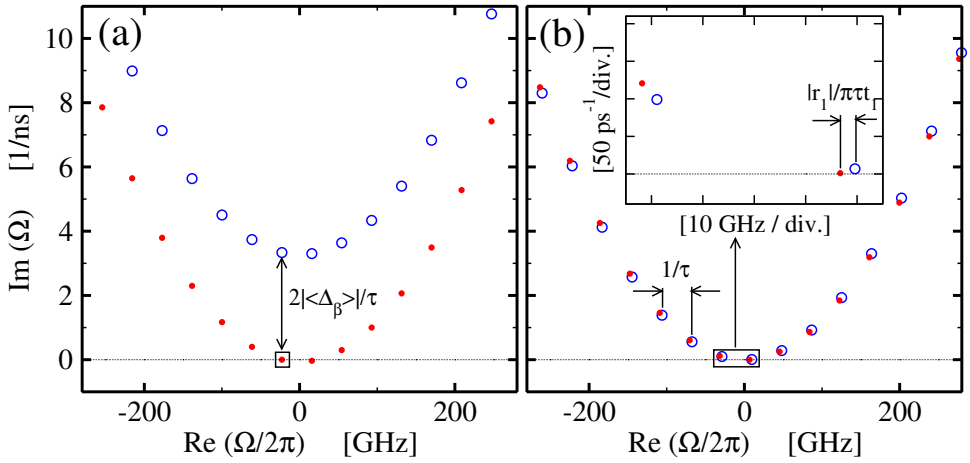

Figure 2: Main roots Ω of Eq. (5) for $r_1 = 0$, $\langle\Delta_\beta\rangle \neq 0$ (a) and $\langle\Delta_\beta\rangle \approx 0$, $r_1 = 0.2$ (b). Other parameters: $\kappa^\pm = \bar{\omega} = 0$, $t_1 = \sqrt{0.7}$, $\tau = 24.666$ ps. Small boxes indicate the modes dominating the dynamical regimes.

Nonuniform spatial distributions of $\beta^\pm$ imply a weak coupling of the optical modes, so that the growth or decay of any mode is slightly influenced by its neighbors [8]. Since the mode coupling decreases with the increasing separation between the complex eigenvalues [9], the strongest mode interaction in the considered ring MSL is between the adjacent k_--th and k_+-th modes. Note also, that a non-vanishing mode coupling permits the existence of neighboring modes with slightly negative $\Im m\,\Omega$ (see Fig. 2(a)), which, however, do not induce instability of the considered states [8]. In the rest of this paper, we analyze the relations of the adjacent modes during dynamical regimes of ring MSLs [2, 5, 7, 10].

A mode with a *real* frequency $\Omega(\beta^\pm) = \bar{\omega}$ and complex factors $s_1'^+$, $s_5''^-$ representing amplitudes of counter-propagating fields at junction J_1 determines any stationary state of the ring MSL. Once $\eta = 10\,\log_{10}(|s_1'^+/s_5''^-|^2)$ is close to zero, we have a bidirectional stationary state. For $|\eta| \gg 0$, the state is unidirectional.

Assume that $r_1 \neq 0$, and the ring MSL operates at a stationary state determined by a mode with the *real* frequency Ω_{k_+} or Ω_{k_-}. Just above threshold the optical fields and the gain saturation are small, so that $\langle\Delta_\beta\rangle \approx 0$. The condition $|\langle\Delta_\beta\rangle| < \Delta_0$ implies the estimate $|\eta| \leq \frac{20\,\Delta_0}{\ln 10}$, which means that the emission intensities at both facets of the out-coupling waveguide should differ by less than 2 dB for $r_1 = 0.2$ and $t_1 = \sqrt{0.7}$ used in Fig. 2(b). Thus, the stationary state at small currents, if present, should be of bidirectional type.

For large currents, the asymmetry $\langle\Delta_\beta\rangle$ can grow, so that $|\langle\Delta_\beta\rangle| > \Delta_0$. Assume that $\langle\Delta_\beta\rangle = i|\langle\Delta_\beta\rangle|$ (i.e. $\nu = 1$), which occurs for dominating E^+ field. The condition $\eta > 0$ (dominance of $s_1'^+$ over $s_5''^-$) is realized by k_+-th mode, i.e., $\Omega_{k_+} = \bar{\omega}$ is real (small bullet on the x-axis of Fig. 2(a)). A non-vanishing r_1 implies an estimate $\eta < 20\log_{10}(t_1/|r_1|)$, what is about 12 dB for r_1 and t_1 discussed above. The complex frequency of the adjacent k_--th mode is given by $\Omega_{k_-} \approx \bar{\omega} + i\frac{2|\langle\Delta_\beta\rangle|}{\tau}$ (see Eq. (6)), i.e., $\Im m\,\Omega_{k_-} > 0$ and this mode is damped (empty bullet just above the small box in Fig. 2(a)). During the switching to the coexisting stationary state determined by the counter-propagating field E^- the factors $\beta^\pm(z)$ change as well. After this switch,

$\langle\Delta_\beta\rangle = -i|\langle\Delta_\beta\rangle|$ (i.e., $\nu = -1$), $\Omega_{k_-}(\beta^\pm) = \bar{\omega}$ and the damping of the previously dominant k_+-th mode is positive again: $\Im m\,\Omega_{k_+} \approx \frac{2|\langle\Delta_\beta\rangle|}{\tau}$. Thus, bistable unidirectional stationary states can be observed in ring MSLs at moderate and high field intensities admitting a well-pronounced asymmetry $\langle\Delta_\beta\rangle$.

Alternating oscillation (AO) of counter-propagating fields of small or moderate intensity is another typical bidirectional dynamic state of ring MSLs. An asymmetry factor in this case is small, $|\langle\Delta_\beta\rangle| \leq \Delta_0$, so that the adjacent mode frequency separation is, approximately, $\frac{2|r_1|}{\tau t_1}$ (see Eq. (6) and Fig. 2(b)). A similar damping and a small mode frequency separation (strong coupling) of a pair of dominant modes suggest a mutual operation (beating) of these modes. The forward (backward) propagating complex optical field at the junction J_1, $E^+(z_1', t)$ ($E^-(z_5'', t)$), can be represented as a sum of two modes with constant in time complex amplitudes $s'^+_{k_\pm,1}$ ($s''^-_{k_\pm,5}$), each rotating with the frequency $\Re e\Omega_{k_\pm}$. Whereas the mode beating (intensity oscillation) frequency $f_{ao} = |\Re e(\Omega_{k_+} - \Omega_{k_-})|/2\pi \approx \frac{|r_1|}{\tau t_1 \pi}$, the phase difference of the oscillating counter-propagating field intensities is given by

$$\phi = \arg\left(\frac{s'^+_{k_+,1}}{s''^-_{k_+,5}}\frac{s'^{+*}_{k_-,1}}{s''^{-*}_{k_-,5}}\right) = 2\,\arg\left(\sinh|\langle\Delta_\beta\rangle| + i\sqrt{\frac{|r_1|^2}{t_1^2} - \sinh^2|\langle\Delta_\beta\rangle|}\right),$$

which converges to π when $\langle\Delta_\beta\rangle \to 0$. Thus, the operation of two adjacent modes suggests f_{ao}^{-1}-periodic anti-phase oscillations of the counter-propagating fields.

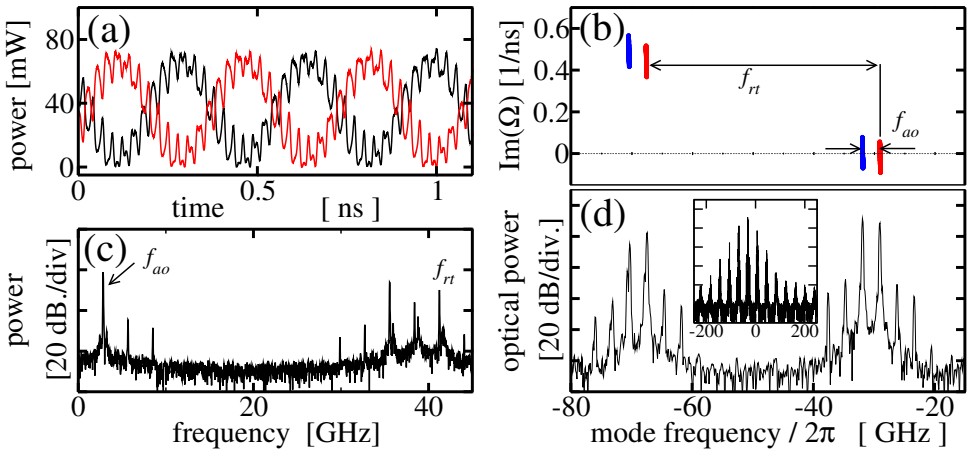

Figure 3: Anti-phase oscillating field intensities $|E_{6,7}^{out}|^2$ in the ring MSL (a), four main $\Omega(\beta^\pm(t))$ at several time instants (b), radio-frequency (c) and optical (d) spectra of E_6^{out}. Parameters as in Fig. 2(b).

The simulations of the ring MSL presented in Fig. 3 confirm our mode analysis. The period of anti-phase oscillating counter-propagating fields (see panel (a)) is determined by the frequency f_{ao} (see panel (c)), which is a separation of the frequencies of the adjacent modes with $\Im m\,\Omega \approx 0$ (panel (b)). The f_{ao}^{-1}-periodic field intensity oscillations presented in panel (a) are additionally modulated with a much higher frequency $f_{rt} \approx |\Omega_{k_\pm} - \Omega_{(k-1)_\pm}|/2\pi \approx \tau^{-1}$ (panel (c)) corresponding to the field round-trip time in the ring cavity. This weak high-frequency modulation is due to additional beating between the main and the neighboring weakly damped side

mode pairs (panel (b)). Finally, the computed mode frequencies (panel (b)) allow us to distinguish between the "real" optical modes and the wave-mixing products in Fourier spectrum of the optical field (panel (d)).

In conclusion, we present an algorithm for location of instantaneous longitudinal optical modes in nearly arbitrary MSL, provided the optical field and carrier dynamics can be adequately described by the 1+1-dimensional TW model. An interpretation of typical observable regimes of ring MSLs performed in this paper reveals the advantages of mode analysis.

Acknowledgements

This work is supported by EU FP7 ITN PROPHET, Grant No. 264687.

References

[1] R. Lang and K. Kobayashi. "External optical feedback effects on semiconductor injection laser properties", *IEEE JQE* **16**, 347–355, (1980)

[2] M. Sorel, G. Giuliani, A. Scire, R. Miglierina, J.P.R. Laybourn, and S. Donati. "Operating regimes of GaAs-AlGaAs semiconductor ring lasers: experiment and model", *IEEE JQE* **39**, 1187–1195, (2003)

[3] E. Gehrig, O. Hess, and R. Walenstein. "Modeling of the performance of high power diode amplifier systems with an optothermal microscopic spatio-temporal theory", *IEEE JQE* **35**, 320–331, (2004)

[4] U. Bandelow, M. Radziunas, J. Sieber, and M. Wolfrum. "Impact of gain dispersion on the spatio-temporal dynamics of multisection lasers", *IEEE JQE* **37**, 183–188, (2001)

[5] J. Javaloyes and S. Balle. "Emission directionality of semiconductor ring lasers: a traveling-wave description", *IEEE JQE* **45**, 431–438, (2009)

[6] A software package LDSL-tool. Longitudinal Dynamics of multisection Semiconductor Lasers. `http://www.wias-berlin.de/software/ldsl`.

[7] M. Radziunas. "Traveling wave modeling of semiconductor ring lasers", *SPIE Proc. Ser.* **6997**, 69971B (2008)

[8] M. Radziunas and H.-J. Wünsche. "Multisection Lasers: Longitudinal Modes and their Dynamics", Chapter 5 in *Optoelectronic Devices: advanced simulation and analysis*, ed. J. Piprek, Springer, 121–150, (2005)

[9] M. Radziunas. "Numerical bifurcation analysis of the traveling wave model of multisection semiconductor lasers", *Physica D* **213**, 98–112, (2006)

[10] A. Pérez-Serrano, J. Javaloyes, and S. Balle. "Bichromatic emission and multimode dynamics in bidirectional ring lasers," *Phys. Rev. A* **81**, 043817 (2010)